Journal of Porous Materials (2023) 30:163–173
https://doi.org/10.1007/s10934-022-01277-3

Natural zeolites as host matrices for the development of low-cost and stable thermochemical energy storage materials

Lia Kouchachvili[1] · D. A. Bardy[1] · Reda Djebbar[1] · LuVerne E. W. Hogg[2]

Accepted: 28 May 2022 / Published online: 20 August 2022

Abstract
Advanced thermal energy storage technologies based on physical adsorption and chemical reactions of thermochemical materials (TCMs) are capable of storing large shares of renewable energy with high energy density. Further research and development is required to improve the performance and reduce the cost of these materials. A promising approach to developing low-cost TCM is to use natural zeolite adsorbents as host matrices in the development of salt-loaded composite TCM. In this study, the thermal properties of various species of low-cost zeolites from natural deposits across Canada were investigated. Two high purity crystal (HPC) zeolites from the Trans Canada (TC-HPC) and Juniper Creek (J-HPC) deposits in British Columbia were determined to have the highest water uptake capacity (0.145 g/g and 0.113 g/g, respectively) and enthalpy of adsorption (408 J/g and 304 J/g, respectively). Despite having approximately half of the water uptake capacity and adsorption enthalpy of the commercially available synthetic zeolite 13X, the cost of thermal energy storage ($CAD/$kWh_{th}$) of the natural zeolites was determined to be 72–79% lower than that of the synthetic zeolite. Repeated adsorption and desorption experiments demonstrated the hydrothermal stability of the HPC zeolites over multiple charge and discharge cycles. Overall, the experimental results and cost analysis indicate that Canadian HPC zeolites are promising alternatives to synthetic zeolites in the pursuit of low-cost and stable TCM.

Keywords Porous matrices · Zeolite · Thermochemical materials · Thermal energy storage · Adsorption

Nomenclature

General Notation

C_Z	Bulk cost of the zeolites ($CAD/tonne)
C_{TES}	Cost of thermal energy storage (kWh_{th})
h_{ads}	Specific enthalpy of adsorption (J/g)
kWh_{th}	Thermal energy (kilo-watt hour)

Abbreviations

BET	Brunauer–Emmett–Teller
CSP	Concentrated solar power
DSC	Differential scanning calorimetry
EDX	Energy dispersive X-ray
HPC	High purity crystal
HVAC	Heating ventilation and air conditioning
RH	Relative humidity
SEM	Scanning electron microscopy
STA	Simultaneous thermal analyser
TCM	Thermochemical energy storage material(s)
TES	Thermal energy storage
TGA	Thermo-gravimetric analysis
XRD	X-ray diffraction
XRF	X-ray fluorescence
SEM	Scanning electron microscopy
EDX	Energy dispersive X-ray

1 Introduction

With increasing demand for renewable energy from intermittent resources such as wind and solar, the development of energy storage technologies is becoming extremely important. Thermal energy storage (TES) technology has the potential to enable the integration of high shares of intermittent renewable energy in the power generation, industrial, and buildings sectors [1].

✉ Lia Kouchachvili
lia.kouchachvili@nrcan-rncan.gc.ca

[1] CanmetENERGY-Ottawa Research Centre, Natural Resources Canada, 1 Haanel Drive, ON K1A 1M1 Ottawa, Canada

[2] ZMM® Canada Minerals Corp., 6459 Mack Road, Peachland, BC V0H 1X8, Canada

Table 1 Selection criteria for TCM used in low-temperature thermochemical TES

Physicochemical properties	Feasibility
Specific surface area and pore volume/size	Capital and operational costs
Heat of sorption and capacity for sorbate	Availability of a local supply
Heat and mass transfer ability	Ease of handling, shaping, and upscaling
Toxicity and environmental impact	
Compatibility with construction materials	
Mechanical durability and hydrothermal stability	

The advancement of TES technologies depends on the development of energy storage materials which are distinguished by the sensible, latent and thermochemical modes of TES. For low-temperature applications including heating and cooling in residential buildings where space for HVAC equipment is highly constrained, thermochemical TES technology based on thermochemical materials (TCM) can offer higher energy storage density (i.e., compactness) and greater temporal flexibility compared to commercialized sensible and latent TES technologies [2]. Instead of storing thermal energy in the change in temperature (sensible) or change in phase (latent) of the storage medium, thermochemical TES systems employ reversible processes including physical adsorption and chemical reactions.

Thermochemical TES systems are able to achieve high energy storage density with negligible heat losses due to the large bonding forces between their working pairs, which typically consists of a solid TCM and water vapour sorbate. Lab-scale prototypes have demonstrated that such systems can be effectively charged by desorbing/dehydrating water from the TCM with heat from solar thermal collectors or electric resistance heaters. The discharge step of thermochemical TES systems is facilitated by reintroducing water vapour to the TCM. The resulting heat of sorption released can be utilized to meet space heating and hot water needs [3–5]. The underlying technology of thermochemical TES is being tested in the laboratory environment and in technical field trials, with much focus on the synthesis and characterization of novel TCMs as the basis of the technology's development [6].

1.1 General TCM characteristics and selection criteria

In a thorough review of solid materials for the application of low-temperature thermochemical TES for space heating in the built environment, Wu et al. highlights the need to consider the suitability of TCM for fulfilling tasks under specific conditions rather than being too prescriptive with the selection approach [7]. Overall, the materials selected or developed for low-temperature thermochemical TES need to ensure high energy storage density while limiting capital and operational costs, and minimizing environmental impact. A high-level list of common selection criteria to consider is included in Table 1.

Solid TCMs are classified as *hygroscopic salts* and *physical adsorbents*—each of which possess particular strengths and weaknesses in the application of thermochemical TES. Most of the hygroscopic salts that were investigated and reported in the literature including $MgCl_2$ and Ca Cl_2, possess high thermal energy storage density (400–600 kWh/m^3) and are relatively low-cost at ≤ $500 USD per metric ton (tonne) [8]. As standalone TCM however, hygroscopic salts can exhibit a behaviour known as deliquescence and melt under certain conditions of temperature and water vapour pressure, resulting in reduced performance of the energy storage system [9, 10].

The most frequently studied physical adsorbents in the literature are zeolite 13X and silica gel. Life cycle analyses considering the required number of cycles of TCMs for the application of TES in residential buildings have concluded that silica gel is not suitable for applications such as seasonal TES [11]. Therefore, we selected 13X zeolite as a reference material. Zeolite 13X (or Na-X)—a synthetic molecular sieve characterized by its high adsorption kinetics for water vapour (water) uptake among traditional adsorbents, especially the binder-free variety [12, 13]. Synthetic zeolites such as binder-free 13X (13XBF) are hydrothermally stable [14]; however, they possess lower energy storage density up to 200 kWh/m^3 [15], at a higher capital cost compared to inorganic salts.[1] Owing to their porous structure, zeolites can be used as matrices to host hygroscopic salts, forming composite "salt in porous matrix" (CSPMs) that utilize both the *ad*sorption enthalpy of the zeolite and the *ab*sorption enthalpy of the salt, resulting in a TCM with improved energy storage density and stability [18]. By using zeolite matrices with different pore structures, and loading them

[1] The bulk cost of commercial zeolite 13X will depend on the supplier and quantity purchased. Market data of annual synthetic zeolite sales suggest an average cost of $2750–$3000 USD per tonne (i.e., ~ $3500 CAD per tonne) based on a global market volume of $450–$550 million USD for 150,000–200,000 tonnes sold up to 2015 [16]. Tran et al. published a weight vs. cost correlation based on commercial data for zeolite 13X, indicating a cost of approximately $6000 CAD per tonne of 13X [17].

Table 2 Natural zeolites received from Canadian companies

Supplier	Name of zeolite sample
ZMM® Canada minerals corp	Trans Canada (TC)-zeolite basalt (ZB) Red (TC-ZB-Red)
	TC- ZB, non-magnetic fraction, high-purity crystals (TC-HPC)
	TC-brown zeolite (TC-BZ)
	British Columbia Heulandite (BC-H)
	Diatomaceous Earth (DE)
	Nova Scotia stilbite (NS-S)
	Juniper zeolite
	US: mordenite/sedimentary (US-M/S) and chabazite/sedimentary (US-Ch/S)
	Nevada clinoptilolite (NV-Clpt)
	Tasajeras cuban clinoptilolite/mordenite (Cuban-Clpt/M)
	Juniper, non magnetic fraction, high-purity crystals (J-HPC)
SECURE energy services, Canada	PZM-Clinoptilolite (PZM-Clpt)
	PZM-Chabazite (PZM-Ch)

with suitable salt hydrates under different synthesis conditions, the resulting composite materials will have different properties tailored to the targeted operational requirements of specific applications.

Superior water uptake and thermal energy storage density has been measured for zeolite 13X loaded with 10–15 wt% salt content [19–23]. Despite their improved performance however, the prices of these developed CSPMs would arguably remain relatively high due to the significant share of synthetic zeolites still used in their composition. On the other hand, according to the U.S. Geological Survey, the price range of natural zeolites sold in the United States was $50–$300 USD per tonne in 2021 [24]. Therefore, at a fraction of the cost of the synthetic variety, natural zeolites are a promising alternative to investigate in the pursuit of developing low-cost CSPMs.

1.2 Natural zeolites as TCM for energy storage

Research on the use of natural zeolites as TCM for the storage of solar thermal energy and heating applications has been of interest for decades due to their physicochemical properties, with both fundamental and applied studies highlighting *chabazite* and *clinoptilolite* as alternatives to synthetic zeolites [25]. More recent studies have focused on the characterization of the thermal properties of natural zeolites [26], including their use in salt-loaded composites [19, 20, 27], with a few applications in lab-scale prototypes [28, 29]. The adsorption properties of natural zeolites may depend on the geographical location of the deposit. That is to say, the measured heat of sorption of samples from a chabazite tuff from Italy [30] may differ from that of a tuff from Russia [31]. Therefore there is a need to test and compare additional zeolite species from different locations, and determine the physicochemical properties for natural zeolites as host matrices for composite TCM development. Similarly, Jänchen et al. studied four zeolite samples of Greek and Serbian origin and determined their different water uptake capacities of 0.14–0.16 g/g [32].

Considering the foregoing motivation, the objective of this work is to investigate the adsorption/desorption properties of a vast amount of Canadian natural zeolite deposits and perform physicochemical analysis to explain their thermal energy storage characteristics. Additionally, a brief analysis was performed to quantify the cost of thermal energy storage associated with the zeolite matrices, providing insight on sizing large-scale thermochemical energy storage systems.

2 Experimental section

2.1 Materials

Samples of natural zeolites were received in different particle sizes from two Canadian companies including SECURE Energy Services, a petroleum service company in Calgary, Alberta, Canada; and, ZMM® Canada Minerals Corp., a minerals research and development company in Peachland, British Columbia, Canada (See Table 2).

A binder-free synthetic zeolite 13X (13XBFK) in form of 1.7–2.5 mm (8 × 12 Mesh ASTM sieve size) diameter spherical beads obtained from Chemiewerk Bad Köstritz GmbH (CWK, Germany) was used as a commercially available benchmark material for comparison to the natural zeolites.

2.2 Methods

Water uptake capacity and the enthalpy of adsorption of the zeolite samples were measured using a simultaneous thermal analyser (STA) which is comprised of a

thermo-gravimetric analyser with differential scanning calorimetry (Netzsch STA 449 F3 Jupiter, Germany). The STA was coupled with a modular humidity generator (MHG). The MHG (ProUmid MHG32, Germany) provided variable water vapour pressure to the specimen in the STA sample holder according to predefined programs for adsorption and desorption of the sample in the STA. Samples in the amount of 10 to 15 mg were first loaded on the STA instrument's sample holder in ceramic crucibles and dried at a defined temperature for two to four hours (depending on the form of material). A water vapour pressure of 1 mbar was selected for the desorption step to mimic ideal conditions for desorption in the built environment. Following desorption, the samples were subject to adsorption conditions of 25 °C under a water vapour pressure of 17 mbar for 4 h. An applied water vapour pressure of 17 mbar at 25 °C using the MHG is equivalent to 53.6% relative humidity (RH). These represent ideal conditions in a lab environment. For a thermochemical TES system operating under cold climate conditions however, the source temperature for evaporation of water may be lower depending on the location and design of the system. A heating rate of 1 °C/min was applied using the furnace of the STA, and a cooling rate of 3 °C/min was applied using compressed air. Nitrogen gas was used as a protective and purge gas at a flow rate of 20 mL/min.

Quantitative elemental composition of the zeolite samples was determined using the Rigaku ZSX Primus II wavelength dispersive-XRF (X-ray Fluorescence) spectrometer. Qualitative X-ray powder diffraction (XRD) was performed to identify crystalline phases present in the zeolite samples. Data was collected using a Rigaku Ultima IV X-ray diffractometer over the angular range 5° to 100° (2θ) 0.01 steps. The XRD system operates in the theta: theta geometry, uses Cu (Kalpha) radiation, 1.5405981 Å, and is equipped with a D/tEX high speed detector. The generator voltage and current settings were 40 kV and 44 mA, respectively. XRD peak search and phase identification were processed using the JADE Standard XRD processing software. Identification of the chemical or mineral compounds was performed using the search/match option in JADE using the ICDD PDF4 + Powder Diffraction Files.

A Micromeritics ASAP 2000 analyzer was used to determine the surface area of the zeolite samples by gas adsorption methods (Brunauer–Emmett–Teller, BET). The 0.5 cm diameter sample pellets were formed with a pelletizer (PIKE Technologies, USA).

The samples were analyzed on a Hitachi S-3400 scanning electron microscopy (SEM) equipped with an Oxford energy-dispersive X-ray (EDX) XMAX detector. EDX data was processed using the Aztec software. Samples were analyzed using an accelerating voltage of 20 kV and a working distance of roughly 10 mm.

3 Results and discussion

3.1 Preliminary screening of zeolites based on their TES capacity

Referring to (b) Fig. 1, the water uptake capacity and the enthalpy of adsorption of all zeolite samples were measured and the two highest adsorbent zeolites were identified. All specimens under the test are in powder form except those with the asterisks in order to see effect of particle size on the adsorption properties of materials in powder versus "as received" granular forms. The numbers appending select samples indicate the ASTM particle size (mesh) in which they were originally received.

The two highest performing zeolites in terms of water uptake and adsorption enthalpy were selected for further investigation and treated as the most suitable matrices for hosting salt hydrates. Referring to the highlighted bars in (b) Fig. 1, these zeolites include TC-HPC and J-HPC, which are from the Trans Canada and Juniper Creek zeolite deposits in British Columbia (Canada), respectively. The stilbite samples from Nova Scotia, Canada (NS-S) were determined to have the lowest water uptake capacity and enthalpy of adsorption. The results of the initial screening investigation are summarized in Table 3. To identify the properties that determine the suitability of zeolites as thermal energy storage materials, further investigation of the selected zeolites' properties were conducted. In the following sections of this paper, the physicochemical properties of the two HPC zeolites are compared to NS-S (demonstrating the lowest TES potential) and 13XBFK (demonstrating the highest TES potential).

The water vapour uptake of TC-HPC and J-HPC natural zeolites were 55% and 43% lower than that of the synthetic zeolite 13XBFK, respectively. There is however a significant difference in the resulting cost of energy storage of using these materials (as will be discussed in Sect. 4), which makes the selected Canadian zeolites compelling candidates as host matrices in composite thermochemical energy storage materials.

3.2 Physical properties of the selected zeolites

Significant differences in the TES capacities of the selected zeolites and the synthetic reference zeolite can be explained by the results obtained from the BET, XRD and XRF analysis (see Table 4, S1 and S2).

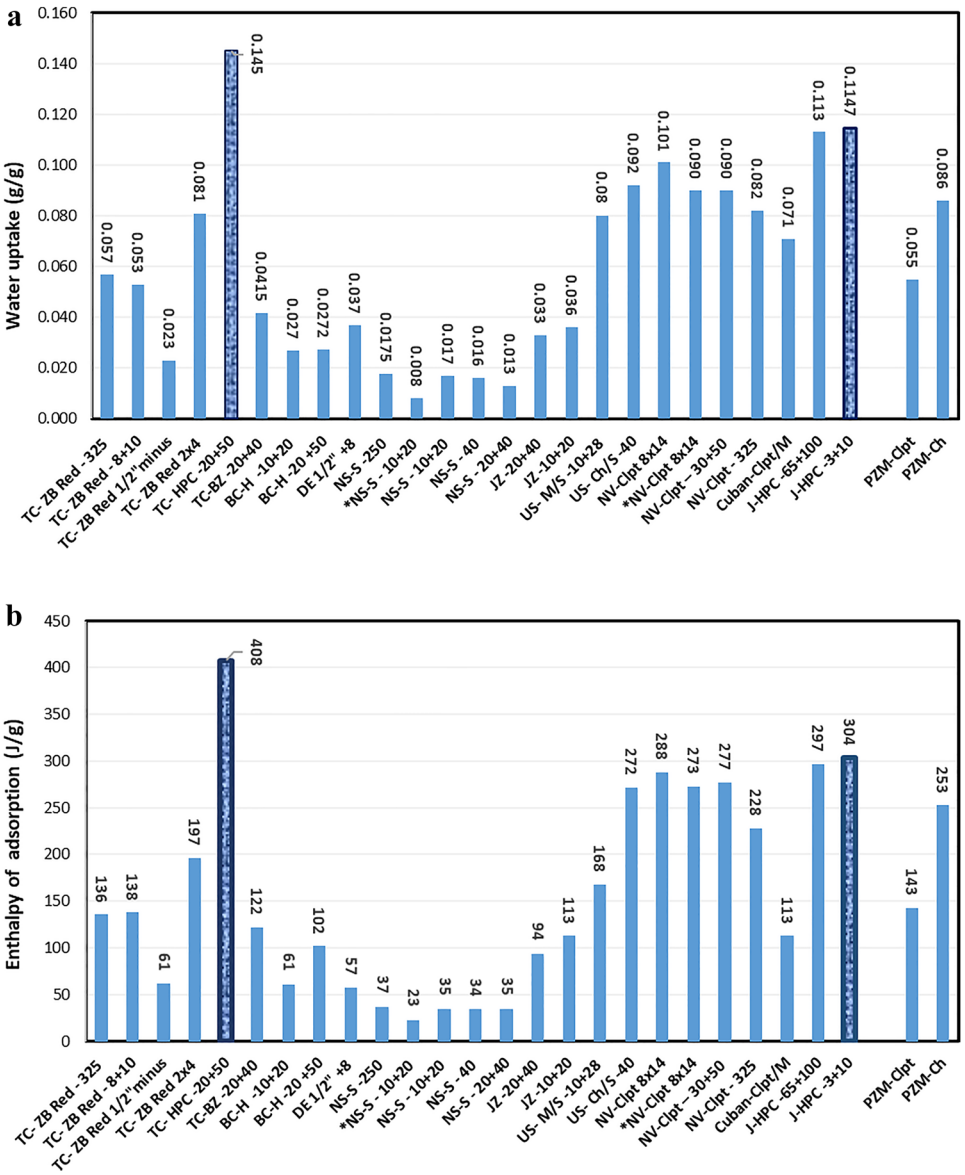

Fig. 1 Water uptake (**a**) and enthalpy of adsorption (**b**) under adsorption conditions of the water vapour pressure of 17 mbar at 25 °C (53.6% RH)

Table 3 Selected zeolites' properties from preliminary screening

Zeolites	Water uptake (g/g)	Enthalpy of adsorption (J/g)	Energy storage capacity (Wh/kg)
13XBFK	0.26	848	236
TC-HPC	0.145	408	113
J-HPC	0.113	304	84
NS-S	0.017	35	10

Table 4 Physical properties of the selected zeolites

Zeolites	BET surface area (m^2/g)	Total pore volume (cm^3/g)	Pore width (Å)	SiO_2/Al_2O_3 (from XRF)
13XBFK	678	0.328	19.34	1.43
TC-HPC	322	0.154	19.14	2.55
J-HPC	294	0.142	19.21	3.06
NS-S	3.72	0.0007	77.5	4.1

The EDX elemental mapping of the selected zeolites are also taken and results are presented in Table 5.

As shown in Table 4, the synthetic zeolite 13XBFK which had the largest surface area and lowest Si/Al ratio performed the best in terms of water uptake and enthalpy of adsorption, whereas the lowest performance was measured for the stilbite, which had the lowest surface area and highest Si/Al ratio. Low surface area and low Al content in stilbite makes it more hydrophobic than other zeolites. Additionally, the stilbite has macro pores and lower pore volumes, therefore

Table 5 EDX analysis results of the selected zeolites

Materials	Average wt%												
	O	Na	Mg	Al	Si	P	S	K	Ti	Ca	Fe	Ni	Ba
13XBFK	47.91	14.50		**16.96**	**19.90**	0.16	0.02		0.35	0.06	0.15		
TC-HPC	52.16	0.17	1.19	**11.18**	**25.94**			2.21		5.45	1.05		0.71
J-HPC	55.36	0.39	2.19	**10.73**	**23.62**			1.35	0.14	4.45	1.78		
NS-S	40.85	0.8	0.75	**5.89**	**20.36**			0.39		3.72	0.97	0.36	21.83

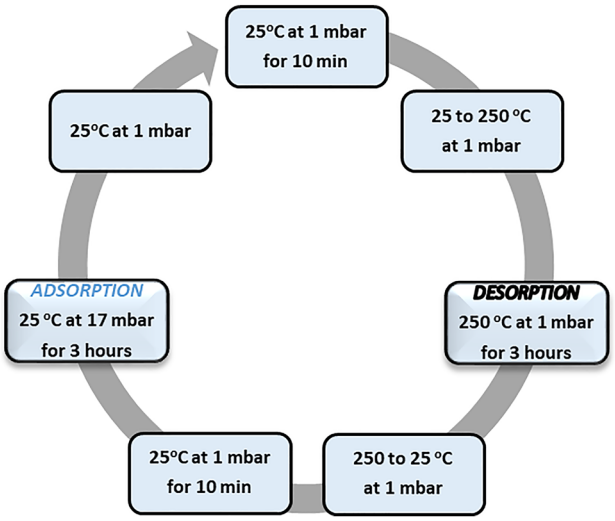

Fig. 2 Schematic of complete desorption/adsorption cycling steps for one cycle

stilbite's water uptake capacity and energy storage capacity are the lowest among the selected zeolites. Detailed XRF and XRD results of the selected zeolite samples have been made available as *Supplementary Inf*ormation.

3.3 Hydrothermal stability of selected zeolites

Whether charged and discharged seasonally or more frequently, it is important to ensure that the TCM installed at the system-level are hydrothermally stable over multiple cycles. Preliminary cycling experiments using the STA were performed over ten desorption/adsorption (i.e., charge/discharge) cycles. The total time for ten cycle hydrothermal stability testing was 133.5 h (see Fig. 2). The sample was initially dried in an air oven for four hours at 250 °C before being loaded in an alumina crucible and subjected to the following iteration of conditions of temperature and water vapour pressure (mbar):

(1) Initial stabilization under 25 °C at 1 mbar for 10 min.
(2) Temperature ramp up to 250 °C (1 °C/min) at 1 mbar.
(3) Temperature soak at 250 °C for 3 h at 1 mbar (*desorption* step).
(4) Temperature ramp down to 25 °C (3 °C/min) at 1 mbar.
(5) Stabilization under 25 °C at 1 mbar for 10 min prior to *adsorption*.
(6) Increase water vapour pressure to 17 mbar at 25 °C (53.6% RH), temperature soak 25 °C for three hours (*adsorption* step).
(7) Decrease water vapour pressure to 1 mbar at 25 °C and repeat cycle, starting at step No. 1.

In general, during the hydrothermal stability test, the results from the first cycle are ignored as the sample is initially dried in the air oven and therefore the first cycle's starting condition is different from the starting conditions of the following cycles. In Fig. 3, the results for the hydrothermal stability test during ten (10) desorption/adsorption cycles for the selected natural zeolites and synthetic 13XBFK are presented.

Referring to Fig. 3, the TES potential in terms of water uptake capacity and enthalpy of adsorption of all zeolites gradually decreased over ten cycles. This is more pronounced for the TC-HPC sample than the J-HPC or 13XBFK samples. The results from the differential scanning calorimetry (DSC) presented in Figs. 4 and 5 show that the enthalpy of adsorption at 9th cycle for the TC-HPC decreases by 38.6% with the comparison to the 2nd cycle (168.2 J/g vs. 274.3 J/g). The J-HPC zeolite shows higher stability (17% decrease, or 392.3 J/g vs. 472.3 J/g) but still much lower stability compared to the 13XBFK zeolite for which a 7% decrease in enthalpy of adsorption between 9th and 2nd cycles was measured (i.e., 614.8 J/g vs. 661.8 J/g).

The desorption/adsorption cycles for J-HPC in the different forms were performed under the same conditions described above. The results are presented in Fig. 6 and Table 6.

It is interesting to see that the water uptake capacity and the enthalpy of adsorption between 2nd and 9th cycles of the granules, unlike powder and pellet, decreases only by 3.0%. However, the physical state of the sample after the test has changed. Visual observation showed that the white crystals of the granules were disintegrated into powder after ten cycles (see Fig. 5d). The pellet's physical appearance stayed the same, however its adsorption capacity reduced by 20.5% at the end of the 9th cycle from the 2nd cycle, which is only 2.7% lower than the decrease in the adsorption capacity of the powder form. Shaped TCM such as pelletized zeolites

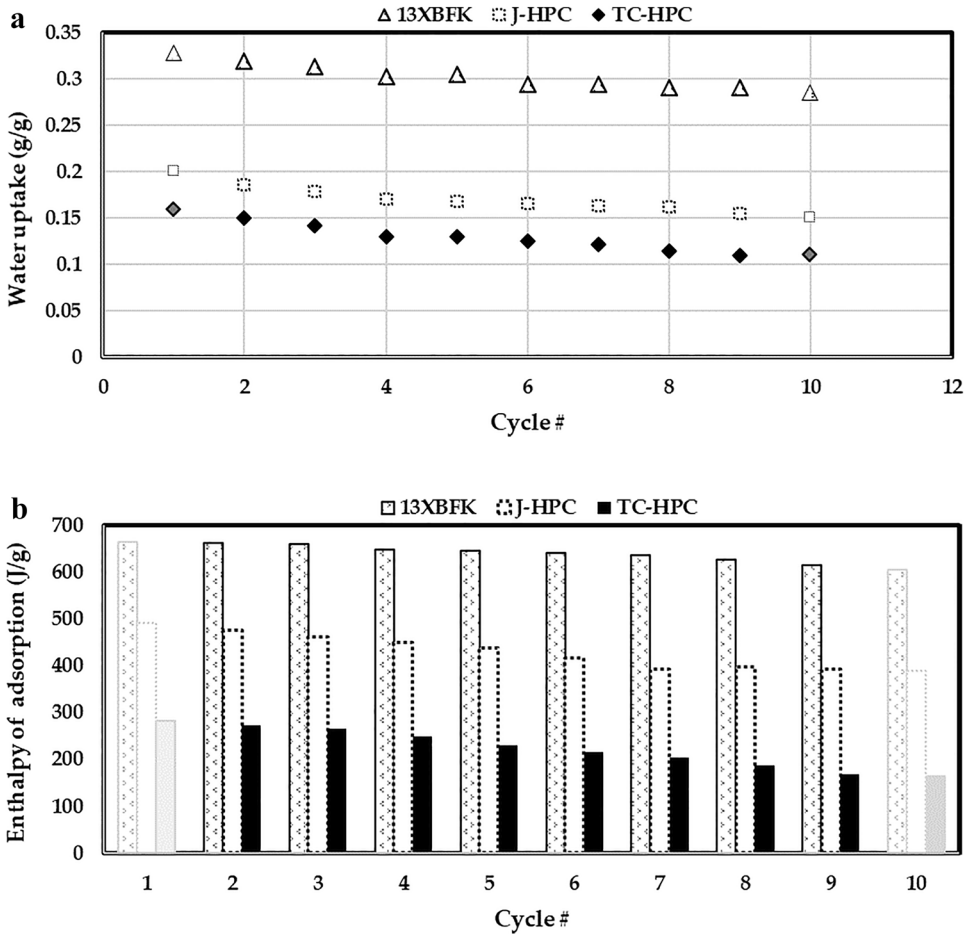

Fig. 3 Evaluation of hydrothermal stability of zeolites in terms of **a** water uptake capacity, and **b** enthalpy of adsorption

are required for practical use at the system-level. Therefore based on this analysis, the J-HPC in pellet form appears to be the best candidate to consider further as a host matrix for stabilizing salt hydrates within its pores.

4 Cost of thermal energy storage analysis

To assess the price reduction potential of using a natural host matrix (vs. synthetic) for further development of high energy storage composite materials, the cost of thermal energy storage (C_{TES}, \$CAD/kWh$_{th}$) of the matrices were calculated using an assumed bulk price of the zeolites[2] (C_Z, \$CAD/tonne) and their corresponding measured heat of adsorption ($h_{ads,}$ J/g) per Eq. 1.

$$C_{TES} = \frac{C_z}{h_{ads}} = \left(\frac{\$}{t}\right) \times \left(\frac{J}{g}\right)^{-1} \times \left|\frac{J}{2.78e^{-7}kWh}\right| \quad (1)$$

The calculated cost of thermal energy storage for ZMM TC-HPC and J-HPC were compared to zeolite 13XBFK which was treated as a benchmark (as noted above) for performance and cost. The numbers in Fig. 7 indicate the cost per unit of thermal energy storage capacity in terms of kWh.

Due to its relatively high bulk price, the estimated current cost of energy storage of 13XBFK (\$25.5 CAD/kWh$_{th}$) was determined to be much greater than that of the J-HPC (\$7.1 CAD/kWh$_{th}$) and TC-HPC (\$5.3 CAD/kWh$_{th}$) zeolites. The lower bulk price of the HPC zeolites resulted in a lower cost of energy storage by 72% (− \$18.4 CAD/kWh$_{th}$) and 79% (− \$20.2 CAD/kWh$_{th}$) for the ZMM J-HPC and TC-HPC, respectively, when compared to 13XBFK.

The National Renewable Energy Lab (NREL, US Department of Energy) has developed a cost model and methodology for estimating the capital cost of TES technologies for the application of high-temperature, utility-scale concentrated solar power systems (CSP) [33]. A target storage cost of \$15/kWh was identified as a goal of the U.S. DOE

[2] For the purpose of this cost analysis, an estimated bulk price of \$6000 CAD per tonne was assumed for the binder-free zeolite 13X tested in this study. ZMM estimated a price of \$600 CAD per tonne for the J-HPC and TC-HPC zeolites, including implicit costs for mining and processing.

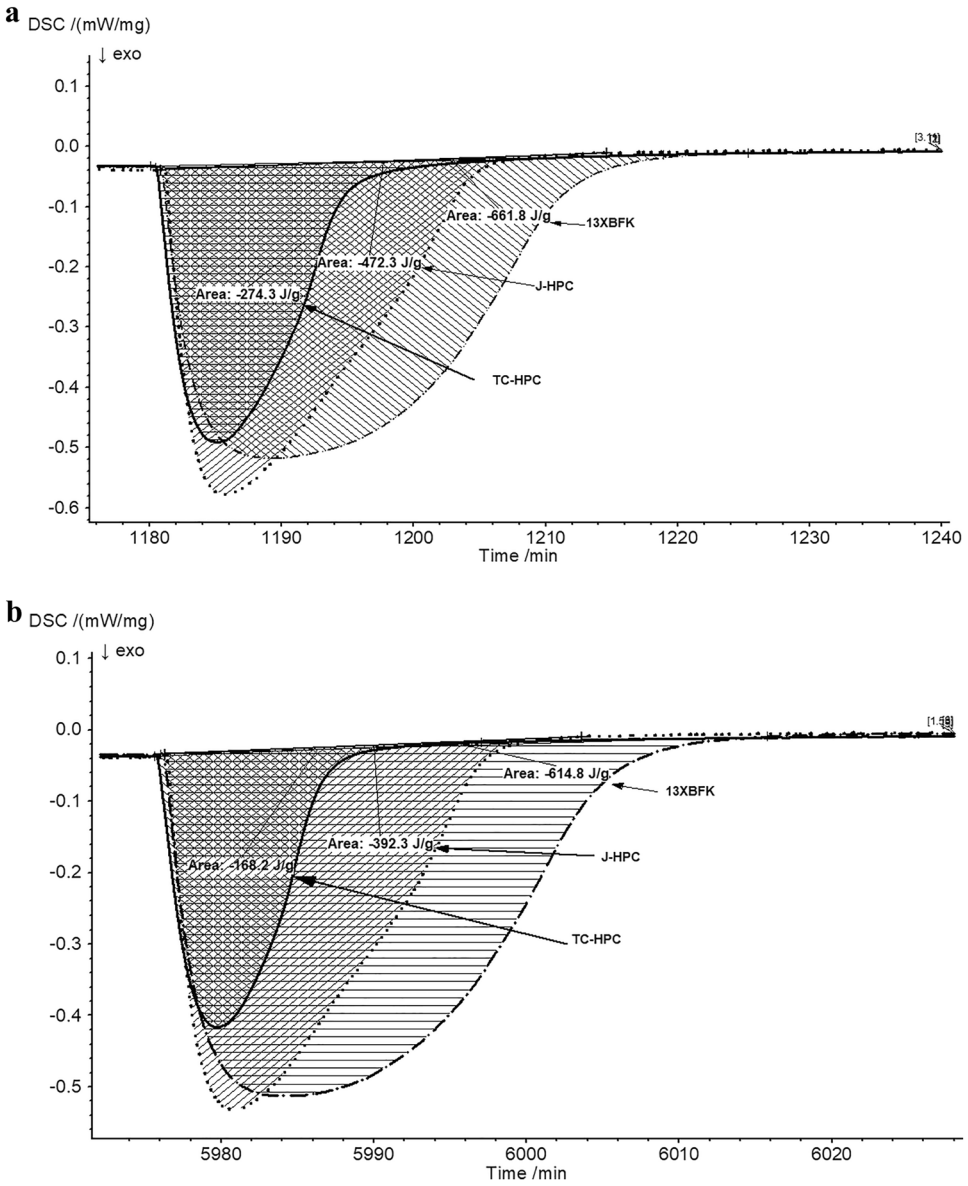

Fig. 4 Images of the DSC graphs for the adsorption steps: **a** second cycle; **b** ninth cycle

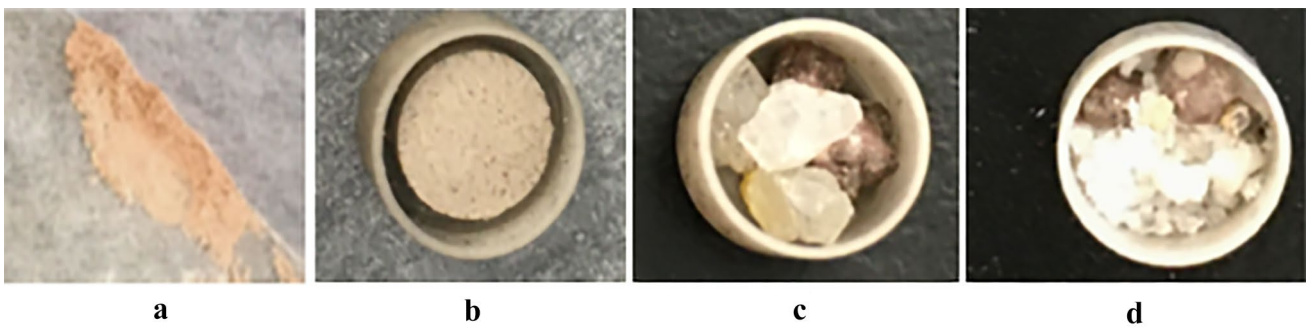

Fig. 5 Photos of the samples in various forms tested, including: **a** powder, **b** pressed pellet, **c** granules, and **d** granules after 10 cycles

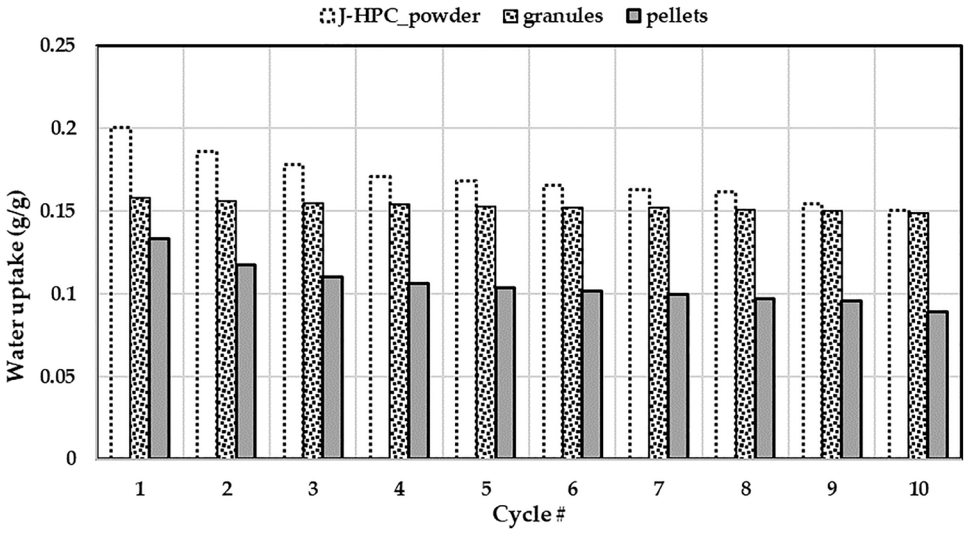

Fig. 6 Hydrothermal stability of the J-HPC zeolite in a different forms: water uptake capacity

Table 6 Hydrothermal stability of the J-HPC zeolite in different forms: enthalpy of adsorption

# of cycles	Enthalpy of adsorption (J/g)		
	powder	granules	pellets
1	491.5	450.8	267.9
2	477.3	452.7	241.8
3	461.9	451.0	227.3
4	450.3	448.8	218.3
5	438.0	448.5	213.6
6	415.9 (17.8%)	445.6 (3.0%)	208.7 (20.5%)
7	393.4	445.5	203.5
8	398.4	444.9	199.2
9	392.5	439.2	192.3
10	389.9	443.0	188.9

SunShot TES Initiative, which includes the cost of materials, sales tax, and contingency costs. While the focus of this present study is on low-temperature TES for building HVAC applications and the determined cost of energy storage is for the TCM only, it is encouraging to see the calculated costs of the HPC fall within the same order of magnitude as the SunShot TES Initiative targets for CSP.

It is important to mention that these results depend on the adsorption conditions imposed on the TCM. For example, decreasing the water vapour pressure of the inlet air would result in a lower heat of adsorption and therefore a higher cost of energy storage. Therefore, the cost of thermal energy storage is constrained by the water vapour pressure and temperature of the evaporator component at the system-level, which poses a challenge for cold climate applications. This challenge will be addressed by the authors in future work using a lab-scale test bench to investigate the use of alternative working fluids to water.

5 Conclusions

The thermal energy storage potential of various species of natural zeolites from Canadian suppliers were characterized in terms of water uptake and enthalpy of adsorption using a simultaneous thermal analyzer coupled with a modular humidity generator. Three samples of natural zeolites were selected for more detailed study based on their thermal performances including: two “high purity crystal” (TC-HPC and J-HPC) zeolites from British Columbia which exhibited encouraging heat storage capacities (408 J/g and 304 J/g respectively), and one stilbite sample from Nova Scotia (NS-S) which showed the poorest performance (35 J/g). These natural zeolite samples were compared to a synthetic binder-free zeolite 13X (13XBFK) as a benchmark to determine which properties influenced performance. The experimental results are in agreement with the results presented in a number of published literature that the water uptake capacity and enthalpy of adsorption of the porous materials are

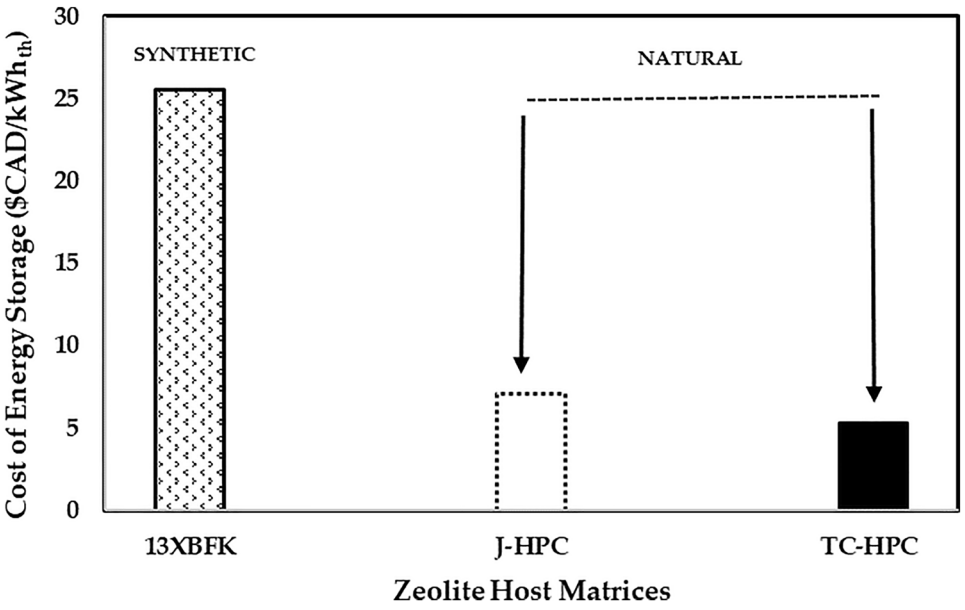

Fig. 7 Calculated cost of thermal energy storage for the top three zeolite candidates studied

proportional to the high surface area, high pore volume of materials and inversely proportional to Si/Al ratio. The natural zeolites ranked from highest to lowest water uptake were TC-HPC > J-HPC > NS-S, corresponding to Si/Al ratios of 2.6, 3.1, and 4.1, respectively. However the higher thermal stability was shown by the J-HPC decreasing by 17% over 8 cycles vs. 38% for TC-HPC. In addition, these selected natural zeolites show a very high cost-effectiveness (< \$7.5 CAD/kWh$_{th}$) when compared to the synthetic reference zeolite 13XBFK (\$25.5 CAD/kWh$_{th}$). Therefore, they are the promising matrices for developing new composite TCMs for TES systems and are currently the subject of further laboratory investigations by the authors.

Supplementary Information The online version contains supplementary material available at https://doi.org/10.1007/s10934-022-01277-3.

Acknowledgements The authors are grateful to Natural Resources Canada's Office of Energy Research and Development (OERD,) for the funding support of this project through the Program for Energy Research and Development (PERD); the Characterization Lab at CanmetENERGY-Ottawa for providing the SEM and elemental analyses; and, ZMM Canada Minerals Corp., SECURE Energy-Alberta, and CWK Germany for providing samples of zeolites tested in this work.

Author contributions LK: Writing—Original Draft, Conceptualization, Methodology, Data Curation, Formal Analysis, Investigation, Visualization. DAB: Writing—Original Draft, Formal Analysis, Investigation, Visualization. RD: Writing—Review & Editing, Supervision, Project Administration, Funding Acquisition. LEWH: Writing—Review & Editing, Resources.

Funding Open Access provided by Natural Resources Canada.

Declarations

Conflict of interest The authors declare that they have no known competing financial interests or personal relationships that could have appeared to influence the work reported in this paper.

References

1. IRENA, Innovation Outlook: Thermal Energy Storage, International Renewable Energy Agency, Abu Dhabi. (2020). https://www.irena.org/publications/2020/Nov/Innovation-outlook-Thermal-energy-storage. Accessed 14 Feb 2022.
2. D. Aydin, S.P. Casey, S. Riffat, Renew. Sustain. Energy Rev. **41**, 356–367 (2015). https://doi.org/10.1016/j.rser.2014.08.054
3. R. Köll, W. van Helden, G. Engel, W. Wagner, B. Dang, J. Jänchen, H. Kerskes, T. Badenhop, T. Herzog, Sol. Energy **155**, 388–397 (2017). https://doi.org/10.1016/j.solener.2017.06.043
4. R. van Alebeek, L. Scapino, M.A.J.M. Beving, M. Gaeini, C.C.M. Rindt, H.A. Zondag, Appl. Therm. Eng. **139**, 325–333 (2018). https://doi.org/10.1016/j.applthermaleng.2018.04.092
5. M. Gaeini, R. van Alebeek, L. Scapino, H.A. Zondag, C.C.M. Rindt, J. Energy Storage **17**, 118–128 (2018). https://doi.org/10.1016/j.est.2018.02.014
6. Y. Zhang, R. Wang, Energy Storage Mater. **27**, 352–369 (2020). https://doi.org/10.1016/j.ensm.2020.02.024

7. H. Wu, F. Salles, J. Zajac, Mol. Basel Switz. **24**(5), 945 (2019). https://doi.org/10.3390/molecules24050945
8. P.A.J. Donkers, L.C. Sögütoglu, H.P. Huinink, H.R. Fischer, O.C.G. Adan, Appl. Energy **199**, 45–68 (2017). https://doi.org/10.1016/j.apenergy.2017.04.080
9. H.A. Zondag, V.M. van Essen, L.P.J. Bleijendaal, B.W.J. Kikkert, M. Bakker, Application of MgCl2·6H2O for thermochemical seasonal solar heat storage, in Presented at the International Renewable Energy Storage Conference IRES 2010, Berlin, Germany, Nov. (2010).
10. L.C. Sögütoglu, M. Steiger, J. Houben, D. Biemans, H.R. Fischer, P. Donkers, H. Huinink, O.C.G. Adan, Cryst. Growth Des. **19**(4), 2279–2288 (2019). https://doi.org/10.1021/acs.cgd.8b01908
11. R. Horn, M. Burr, D. Fröhlich, S. Gschwander, M. Held, Procedia CIRP **69**, 206–211 (2018). https://doi.org/10.1016/j.procir.2017.11.095
12. B. Mette, H. Kerskes, H. Drück, H. Müller-Steinhagen, Int. J. Heat Mass Transf. **71**, 555–561 (2014). https://doi.org/10.1016/j.ijheatmasstransfer.2013.12.061
13. M. Gaeini, H.A. Zondag, C.C.M. Rindt, Appl. Therm. Eng. **102**, 520–531 (2016). https://doi.org/10.1016/j.applthermaleng.2016.03.055
14. G. Storch, G. Reichenauer, F. Scheffler, A. Hauer, Adsorption **14**, 275–281 (2008). https://doi.org/10.1007/s10450-007-9092-7
15. D. Dicaire, F.H. Tezel, Renew. Energy **36**(3), 986–992 (2011). https://doi.org/10.1016/j.renene.2010.08.031
16. K. Gleichmann, B. Unger, A. Brandt, in *Zeolites—Useful Minerals*. ed. by C. Belviso (IntechOpen, London, 2016). https://doi.org/10.5772/63442
17. T.V. Tran, A.O. Oni, E. Gemechu, Y. Carrier, F.H. Tezel, A. Kumar, Energy Convers. Manag. **244**, 114325 (2021). https://doi.org/10.1016/j.enconman.2021.114325
18. Y.I. Aristov, *Nanocomposite Sorbents for Multiple Applications* (Jenny Stanford Publishing, Singapore, 2020)
19. G.T. Whiting, D. Grondin, S. Bennici, A. Auroux, Sol. Energy Mater. Sol. Cells **112**, 112–119 (2013). https://doi.org/10.1016/j.solmat.2013.01.020
20. G.T. Whiting, D. Grondin, D. Stosic, S. Bennici, A. Auroux, Sol. Energy Mater. Sol. Cells **128**, 289–295 (2014). https://doi.org/10.1016/j.solmat.2014.05.016
21. T. Nonnen, S. Beckert, K. Gleichmann, A. Brandt, B. Unger, H. Kerskes, B. Mette, S. Bonk, T. Badenhop, F. Salg, R. Gläser, Chem. Eng. Technol. **39**(12), 2427–2434 (2016). https://doi.org/10.1002/ceat.201600301
22. S.Z. Xu, S. Lemington, R.Z. Wang, L.W. Wang, J. Zhu, Energy Convers. Manag. **171**, 98–109 (2018). https://doi.org/10.1016/j.enconman.2018.05.077
23. D. Mahon, P. Henshall, G. Claudio, P.C. Eames, Renew. Energy **145**, 1799–1807 (2020). https://doi.org/10.1016/j.renene.2019.05.135
24. R. D. Crangle, Jr., Mineral Commodity Summaries 2022: Zeolites (Natural). U.S. Geological Survey. (2022). https://doi.org/10.3133/mcs2022
25. D.I. Tchernev, Rev. Mineral. Geochem. **45**(1), 589–617 (2001). https://doi.org/10.2138/rmg.2001.45.17
26. J. Jänchen, H. Stach, U. Hellwig, in *Studies in Surface Science and Catalysis*, vol. 174, ed. by A. Gédéon, P. Massiani, F. Babonneau (Elsevier, Amsterdam, 2008), pp. 599–602. https://doi.org/10.1016/S0167-2991(08)80271-6
27. G. Issayan, B. Zettl, W. Somitsch, in Proceedings of the 14th International Renewable Energy Storage Conference 2020 (2021), pp. 49–57. https://doi.org/10.2991/ahe.k.210202.008
28. B. Zettl, G. Englmair, W. Somitsch, Energy Procedia **73**, 297–304 (2015). https://doi.org/10.1016/j.egypro.2015.07.692
29. S. Nasruddin, A.P. Arsyad, S. Djubaedah, D.A. Wulandari, H.F. Hidayat, AIP Conf Proc **2255**(1), 040036 (2020). https://doi.org/10.1063/5.0013934
30. R. Aiello, A. Nastro, G. Giordano, C. Colella, Solar energy storage by natural zeolites II. Activation and heat recovery in open systems, in *Occurrence, Properties and Utilization of Natural Zeolites*, Budapest, Hungary: Akademiai Kiado (1988), pp. 763–772.
31. G.P. Valueva, I.A. Belitsky, Y.V. Seryotkin, V.S. Pavlychenko, Natural chabazite: heats of rehydration and X-ray study in relation to H2O contents at room temperature, in Occurrence, Properties and Utilization of Natural Zeolites, Budapest, Hungary: Akademiai Kiado (1988), pp. 283–289.
32. J. Jänchen, T.H. Herzog, E. Thrun, Natural zeolites in thermal adsorption storage and building materials for solar energy utilization in houses, in Presented at the SASEC2015, Kruger National Park, South Africa, May 2015.
33. G. Glatzmaier, *Developing a Cost Model and Methodology to Estimate Capital Costs for Thermal Energy Storage* (National Renewable Energy Lab, Golden, 2011). https://doi.org/10.2172/1031953